MoS_2 quantum dots: synthesis, properties and biological applications

Yongming Guo,[a,*] Jianwei Li,[b,*]

[a]Collaborative Innovation Center of Atmospheric Environment and Equipment Technology, Jiangsu Key Laboratory of Atmospheric Environment Monitoring and Pollution Control, Jiangsu Engineering Technology Research Center of Environmental Cleaning Materials, School of Environmental Science and Engineering, Nanjing University of Information Science & Technology, Nanjing 210044, China

[b]Department of Chemistry, University of Turku, Vatselankatu 2, Turku 20014, Finland

*Corresponding author.

E-mail addresses: chinahenangm@163.com (Yongming Guo); jianwei.li@utu.fi (Jianwei Li)

Abstract:

Fluorescent nanomaterials have gained momentum due to their specific properties and promising applications in various fields. Molybdenum disulfide quantum dots (MoS_2 QDs) are emerging as a new class of fluorescent nanomaterials that have generated tremendous research interests due to their unique optical properties and good biocompatibility. In this review, we firstly present an overview of the significant advances of MoS_2 QDs in synthetic strategies including top-down and bottom-up approaches, followed by discussing their distinctive properties. Then, the detailed biological applications of MoS_2 QDs are provided. Finally, the challenges and perspectives of MoS_2 QDs based materials are indicated as well.

Keywords: MoS_2 quantum dots; synthesis; properties; biological applications

1. Introduction

Over the last few years, two-dimensional (2D) transition-metal dichalcogenide nanomaterials have attracted considerable research interests due to their fascinating properties including optical properties, electrochemical and catalytic activities. As a consequence, many promising applications in sensing, photocatalysis, energy, biomedicine and other related fields have been demonstrated [1-5]. Once these 2D nanomaterials suffered subsequent treatment, their size would be further decreased, yielding quantum dots with unique optical properties exhibiting plenty of applications in a variety of fields. Among these transition-metal dichalcogenide quantum dots, molybdenum disulfide quantum dots (MoS_2 QDs) have gained tremendous attention over many fields due to their ease of fabrication and good biocompatibility. And as compared with other morphologies of MoS_2 nanostructures including nanosheets and nanotubes, MoS_2 QDs exhibited small size and tunable fluorescence emission, which endow them with promising applications in biology, such as biosensing, bioimaging, and so on. Up to now, various techniques have been developed for the synthesis of MoS_2 QDs including top-down and bottom-up approaches. Meanwhile, numerous applications of MoS_2 QDs have been explored in many areas including sensing, electrocatalysis, bioimaging, energy and so on [6]. However, so far there has been only one review about the synthesis and applications of MoS_2 QDs, also the properties and detailed biological applications of MoS_2 QDs have not been reviewed yet. Therefore, a comprehensive review about the progress of MoS_2 QDs is highly desirable.

In this review, we will introduce the advances of synthesis, properties and the biological applications of MoS_2 QDs. In the first section, the synthetic strategies of MoS_2 QDs will be presented, which can be categorized into top-down and bottom-up methods. The top-down approaches mainly include chemical exfoliation, mechanical exfoliation, electrochemical method, emulsion method, solvothermal method, thermal ablation method and combined method. Compared with the numbers of types of top-down approaches, the bottom-up methods are rare. Hydrothermal method is the only way that has been developed to make MoS_2 QDs from the bottom-up side.

Yet, the hydrothermal method is commonly utilized for preparing various functionalized MoS_2 QDs with many applications due to their simplicity and good repeatability. In the second section, the unique properties of MoS_2 QDs are exhibited, including absorbance, fluorescence, electrocatalytic activities, toxicity and quantum yield (QY). In the third section, the detailed biological applications of MoS_2 QDs in biosensing, bioimaging, phototherapy and drug delivery are summarized. In the end, we will point out the challenges and perspectives of MoS_2 QDs in synthesis and biological applications. We expect that the review will give insights into new development of MoS_2 QDs and lead to innovations for the synthesis and promising biological applications.

2. Synthesis of MoS_2 QDs

Over the past decades, continuous efforts have been devoted to developing a variety of strategies for synthesizing MoS_2 QDs with different properties. The synthetic approaches of MoS_2 QDs are mainly divided into top-down and bottom-up methods. In the top-down approach, various techniques were utilized to treat bulk MoS_2 into MoS_2 QDs with smaller size. As a consequence, chemical exfoliation, mechanical exfoliation, electrochemical method, emulsion method, solvothermal method, thermal ablation method and combined method have been well constructed for the fabrication of MoS_2 QDs (**Figure 1**). However, the bottom-up technique only means hydrothermal method for synthesizing MoS_2 QDs, in which different molybdenum sources and various sulfur sources are hydrothermally treated at reaction vessels to form MoS_2 QDs (**Figure 1**).

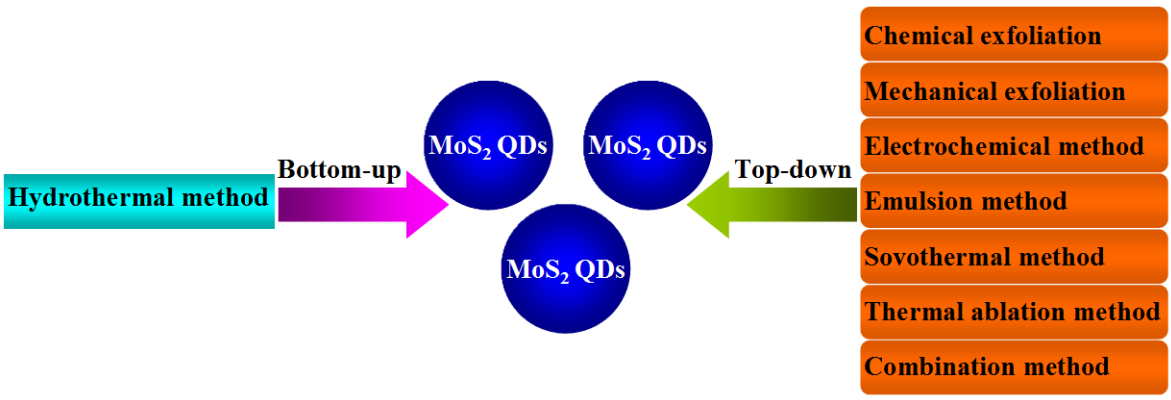

Figure 1. Synthetic approaches of MoS_2 QDs.

2.1. Top-down

2.1.1 Chemical exfoliation

Chemical exfoliation is a common approach for the synthesis of MoS_2 QDs from bulk MoS_2 through reversibly inserting foreign species at the crystal gaps. Zhou and co-workers have developed a chemical intercalation and exfoliation process from bulk MoS_2 by metal Na at 160 °C in a Pyrex tube under vacuum. The method does not require any organic reagents and further treatment. The as-prepared MoS_2 QDs displayed blue emission with maximum at 430 nm and excitation-dependent emission behavior. And the MoS_2 QDs with QY of 11% exhibited good photostability, low cytotoxicity, which were used to image in HeLa cells [7].

Lithium (Li) intercalation has also been utilized for exfoliation of bulk MoS_2 into MoS_2 QDs. Zhong's group has proposed a multi-exfoliation method based on Li intercalation for the synthesis of MoS_2 QDs. Taking the advantage of the weak interlayer van der Waals force, Li^+ was intercalated bulk MoS_2, forming Li-intercalated MoS_2. After multi-exfoliation and purification, MoS_2 QDs were obtained. The cutting mechanism of MoS_2 QDs may be attributed to the complete breakup around the defects and edges during the reaction of Li_xMoS_2 with water and its following ultrasonication process. The high content of Li^+ in bulk MoS_2 can yield some defects, which may make MoS_2 nanosheets fragile and easily lead to the formation of MoS_2 QDs. The as-prepared MoS_2 QDs showed weak blue fluorescence owing to the existence of 1T phase. However, heating treatment could further boost the fluorescence intensity excited at 300 nm by five times. And the MoS_2 QDs solution exhibited an excitation-dependent emission behavior (**Figure 2A**) [8]. The chemical exfoliation has been successfully utilized for effectively preparation of MoS_2 QDs, yet it required complicated operations and the addition of foreign ions, as well as the performance of MoS_2 QDs is not perfect.

2.1.2 Mechanical exfoliation

Ultrasound is an effective mechanical approach for the exfoliation of bulk MoS_2 into MoS_2 QDs. Generally, monolayered MoS_2 nanosheets could be obtained after the treatment of natural mineral molybdenite with intensive ultrasound in a pressurized

batch reactor. And MoS_2 QDs could be easily fabricated through refluxing the monolayered MoS_2 nanosheets in ethylene glycol at atmospheric pressure for 24 hours. Ultrasonic power could exfoliate bulk MoS_2 into MoS_2 nanosheets, which could be further broken into blue-emitting MoS_2 QDs after refluxing in ethylene glycol for 24 hours. The work offered an effective and facile approach for exfoliation of other layered materials [9]. Dai *et al*. developed a sulfuric acid assisted ultrasonic method for synthesizing MoS_2 QDs by exfoliating and cutting bulk MoS_2. With the assistance of ultrasonication, sulfuric acid molecule could intercalate into the layers of MoS_2, which could be exfoliated into single-layer MoS_2 flake, and MoS_2 flake was further cut into small size of MoS_2 QDs (**Figure 2B**). The resulting MoS_2 QDs with strong blue emission displayed excellent excitation-independent emission behavior. Interestingly, the multiphoton bioimaging of MoS_2 QDs was demonstrated in HeLa and HaCaT cells [10].

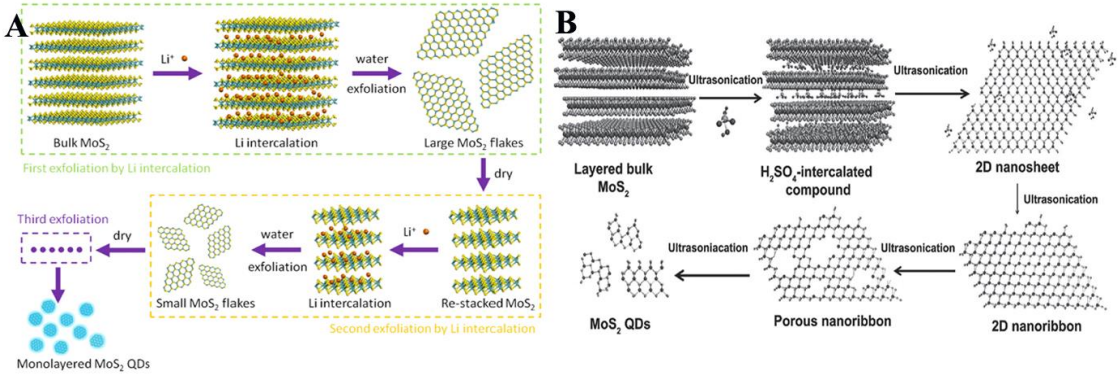

Figure 2. Schematic illustration of the synthesis of MoS_2 QDs via chemical exfoliation (A) and mechanical exfoliation (B). A: Reprinted with permission from [8]. Copyright (2015) Elsevier. B: Reprinted with permission from [10]. Copyright (2015) Wiley-VCH.

2.1.3 Electrochemical method

Electrochemical method is a cost-effective and eco-friendly technique for preparing MoS_2 QDs. A one-step electrochemical method has been utilized for the synthesis of MoS_2 QDs from its bulk material in aqueous ionic liquid solution of 1-butyl-3-methylimidazolium chloride ([BMIm]Cl) and lithium bis-trifluoromethylsulphonylimide (LiTFSI). MoS_2 QDs with different size were

achieved in different concentrations of LiTFSI or [BMIm]Cl under the condition of a constant direct current potential of 5 V in a two-electrode cell. The generation of free radicals in the electrochemical procedure could trigger the initial cleavage and lead to further exfoliation of the bulk material, resulting in the formation of MoS_2 QDs (**Figure 3A**). The fluorescence spectra of MoS_2 QDs exhibited broad emission at about 400 nm, and the excitation-dependent emission characteristic was also observed. The as-prepared MoS_2 QDs have been also demonstrated to exhibit excellent electrocatalytic activities towards hydrogen evolution reaction [11]. Li's group has proposed an electrochemically induced Fenton reaction for synthesizing MoS_2 QDs. In the electro-Fenton process, the Fenton reagent from electrochemical generation of H_2O_2 and added Fe^{2+} could generate hydroxyl radicals, which could etch MoS_2 nanosheets into MoS_2 QDs with optimal emission peak at 370 nm (**Figure 3B**). And the obtained MoS_2 QDs exhibited excitation-dependent and pH-dependent emission behavior [12].

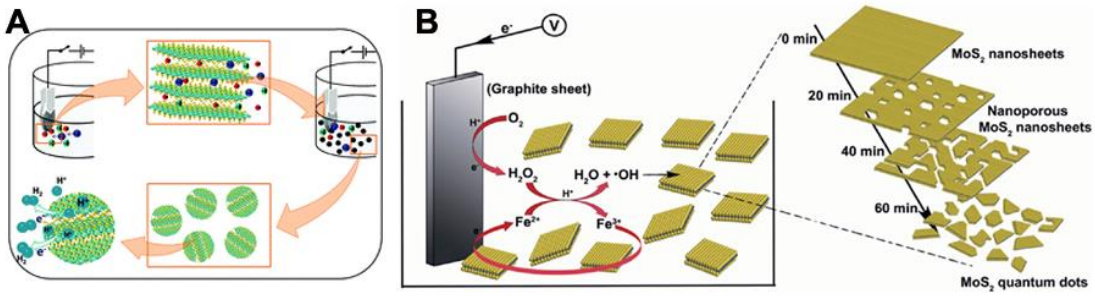

Figure 3. (A) Illustration of electrochemical method for synthesizing MoS_2 QDs from its bulk materials in aqueous ionic liquid solutions of [BMIm]Cl and LiTFSI. Reprinted with permission from [11]. Copyright (2015) the Royal Society of Chemistry. (B) Scheme of electrochemically induced Fenton reaction approach for synthesis of MoS_2 QDs from MoS_2 nanosheets. Reprinted with permission from [12]. Copyright (2014) the Royal Society of Chemistry.

2.1.4 Emulsion method

MoS_2 QDs can be also prepared in the microenvironment of emulsions built by the water/surfactant/CO_2 system. Nonionic polyvinylpyrrolidone (PVP), a water-soluble and biocompatible polymer, was utilized in the system, which could adsorb on the

surface of MoS_2 nanosheets owing to the excellent wetting property and 2D plane structure. Supercritical CO_2 was used to help build the microenvironment of emulsions and tune the phase behavior. MoS_2 powder was dissolved in the microenvironment of emulsions, and was further put into the autoclave for reaction 3 hours at 313.2 K and the desired pressure (16 MPa) was produced from CO_2. After ultrasound and centrifugation, MoS_2 QDs were obtained, which exhibited polydispersity of the lateral dimensions. MoS_2 QDs showed excitation-dependent fluorescence behavior, revealing their potential applications in optoelectronics and biology [13].

2.1.5 Solvothermal method

Solvothermal method is a simple approach for the synthesis of MoS_2 QDs without using any strong acid or surface passivation reagent. In the presence of NaOH, MoS_2 QDs were successfully prepared via the solvothermal treatment of MoS_2 powder in ethanol solution. The ethanol solution could boost the contact interface between hydrophobic MoS_2 and NaOH. NaOH could corrode the edges of MoS_2, and Na^+ and OH^- could insert between the MoS_2 layers, which could exfoliate MoS_2 layer by layer, further break into MoS_2 QDs. The obtained MoS_2 QDs with high crystallinity exhibited bright blue fluorescence, excitation-dependent emission feature and excellent biocompatibility, demonstrating a facile approach for large-scale production of MoS_2 QDs (**Figure 4A**) [14]. Similarly, Wu's group reported a simple solvothermal treatment of MoS_2 powder for preparing MoS_2 QDs in N,N-dimethylformamide. The as-prepared MoS_2 QDs with average size of approximately 3.9 nm displayed strong blue fluorescence with maximum emission at 463 nm. Also, the method was suitable for the synthesis of WS_2 QDs and MoS_2/WS_2 QDs [15].

2.1.6 Thermal ablation method

Thermal ablation method is a physical strategy for the fabrication MoS_2 QDs without using any solvent. Kim's group constructed a thermal annealing technique for synthesis of MoS_2 QDs. Single layer MoS_2 formed from chemical vapor deposition was applied as a precursor to suffer from thermal annealing at 500 °C for 70 h, producing MoS_2 QDs with 4-7 nm. The fluorescence spectra displayed a blue shift

from 682 nm to 548 nm because of the quantum confinement effects across the 2D planes [16]. The work provides an efficient method for the fabrication of MoS_2 QDs in large scale. Still, the performance of MoS_2 QDs is highly needed to improve.

2.1.7 Combined method

To exploit more effective methods for preparing MoS_2 QDs, various combined methods were developed. Xian's group presented a combined method of ultrasonication and ethanol-thermal treatment of MoS_2 powder for the synthesis of blue-emitting MoS_2 QDs. The combination of ultrasonication and ethanol-thermal method could effectively break bulk MoS_2 into MoS_2 QDs. The MoS_2 QDs showed small size, high stability and two photon fluorescence property, which were successfully utilized for cell imaging [17]. And a sonication combined with ion intercalation method was proposed to prepare MoS_2 QDs with variable fluorescent emission. In the formation of MoS_2 QDs, sonication in N-methylpyrrolidone (NMP) could lead to the formation of MoS_2 nanosheets and a small amount of MoS_2 QDs. And the addition of alkali metal ions in the sonication process could improve the efficiency of exfoliation, yielding MoS_2 QDs (**Figure 4B**). The MoS_2 QDs exhibited variable fluorescent emission at different excitation wavelengths, which is promising in optoelectronic field and cell imaging. And the QY could be increased to 4.84% from 0.99% after the addition of sodium hydroxide [18]. Ali *et al*. fabricated a blue-emitting MoS_2 QDs via wet grinding assisted co-solvent sonication strategy, in which pristine MoS_2 was first wet grinded in NMP assisted bath and treated with probe sonication in NMP and 1,2-dichlorobenzene, resulting in formation MoS_2 QDs with 2-5 nm in size. The obtained MoS_2 QDs showed a distinguished blue emission at 448 nm [19].

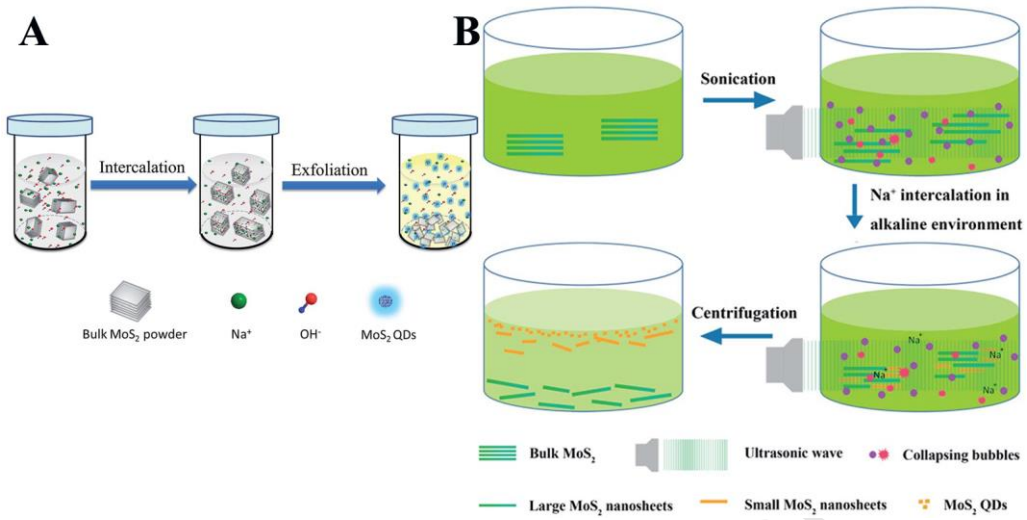

Figure 4. Schematic illustration of the synthesis of MoS_2 QDs via solvothermal method (A) and combined method (B). A: Reprinted with permission from [14]. Copyright (2016) the Royal Society of Chemistry. B: Reprinted with permission from [18]. Copyright (2015) the Royal Society of Chemistry.

2.2 Bottom-up

Bottom-up approach is one of the most used approaches to synthesize a variety of nanomaterials by using huge number of precursors which are usually small molecules. The current bottom-up method for the fabrication of MoS_2 QDs is hydrothermal method by using different molybdate sources and sulfur-containing small molecules. The sulfur-containing small molecules serve as reducing agents to reduce various molybdate sources, resulting in the formation of MoS_2 QDs. Compared to those exfoliation strategies, the hydrothermal approach is simple and eco-friendly without requirement complicated operations. Also, the size and fluorescent properties of MoS_2 QDs could be easily controlled by altering the precursors or experimental conditions. Wang and Ni recently synthesized MoS_2 QDs through hydrothermal treatment of sodium molybdate and L-cysteine (L-Cys) at 200 ^{o}C for 36 hours. The as-prepared MoS_2 QDs with QY of 2.6% showed excitation-dependent emission behavior with a maximum emission wavelength at 402 nm [20]. Similarly, glutathione (GSH) [21], dibenzyldisulfides [22], thiourea [23], thioglycolic acid and sodium sulfide [24, 25], N-acetyl-L-cysteine (NAC) [26] have been employed to synthesize MoS_2 QDs with various molybdate as precursor (**Figure 5**). A hydrothermal method has been

proposed for synthesizing MoS_2 QDs through the reduction of $(NH_4)_2MoS_4$ by N_2H_4 (**Figure 5**). The resulting MoS_2 QDs with maximum emission at about 400 nm also exhibited excitation-dependent emission behavior and pH-dependent fluorescence property [27]. Meanwhile, oleylamine could be also utilized as a reducing agent for the preparation of MoS_2 QDs when using $(NH_4)_2MoS_4$ as a precursor (**Figure 5**). The obtained MoS_2 QDs with QY of 4.4% showed the optimal emission at 575 nm and excitation-dependent emission feature [28].

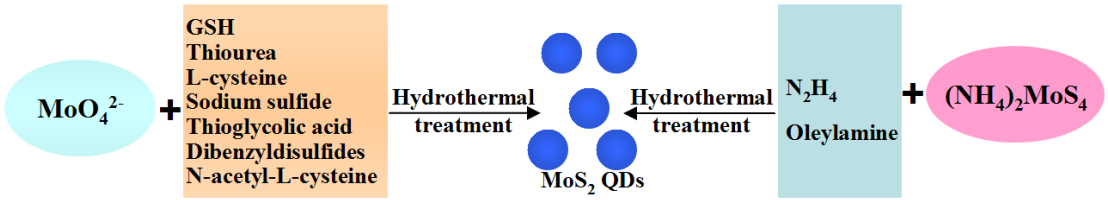

Figure 5. Illustration of hydrothermal approach for synthesizing MoS_2 QDs from different precursors.

The above mentioned approaches have been utilized to prepare MoS_2 QDs with various properties. To make it easier for the readers to compare the performance of these synthetic methods of MoS_2 QDs, a summary concerning their advances was presented in **Table 1**.

Table 1 List of different synthetic methods for MoS_2 QDs

Method	Precursors	QY	Emission	Reference
Chemical exfoliation (Na intercalation)	Bulk MoS_2 powder	11%	430 nm	[7]
Chemical exfoliation (Li intercalation)	2H-MoS_2 powder	-	420 nm	[8]
Mechanical exfoliation-ultrasound method	Natural molybdenite	-	~480 nm	[9]
Mechanical exfoliation -sulfuric acid assisted ultrasonic method	MoS_2 powder	9.65%	414 nm	[10]
Electrochemical method	Bulk MoS_2 powder	-	~400 nm	[11]
Electrochemical method	MoS_2 nanosheets		401 nm	[12]
Emulsion method	MoS_2 powder	-	~ 480-540 nm	[13]
Solvothermal method	MoS_2 powder	-	461 nm	[14]
Solvothermal method	MoS_2 powder	-	463 nm	[15]
Thermal ablation method	Single layer MoS_2	-	548 nm	[16]
Combined method (Ultrasonication+ ethanol-thermal method)	MoS_2 powder	3.1%	428 nm	[17]
Combined method (Sonication+ion intercalation method)	MoS_2 powder	4.84%	~500 nm	[18]

Combined method (Wet grinding+co-solvent sonication)	MoS_2 powder	-	448 nm	[19]
Hydrothermal method	Sodium molybdate+L-cysteine	2.6%	402 nm	[20]
Hydrothermal method	Sodium molybdate+glutathione	~ 10.3%	425 nm	[21]
Hydrothermal method	Sodium molybdate+dibenzyldisulfides	-	280 nm	[22]
Hydrothermal method	Sodium molybdate+thiourea	0.28%	406 nm	[23]
Hydrothermal method	Molybdenyl acetylacetonate+thioglycolic acid+Na_2S	-	420 nm	[24]
Hydrothermal method	Sodium molybdate+Na_2S+1,4-Diaminobutane		423 nm	[25]
Hydrothermal method	Ammonium molybdate+N-acetyl-L-cysteine+thiourea	-2%	480 nm	[26]
Hydrothermal method	$(NH_4)_2MoS_4$+N_2H_4	-	400 nm	[27]
Hydrothermal method	$(NH_4)_2MoS_4$+oleylamine	4.4%	575 nm	[28]

3. Properties

MoS_2 QDs with good water solubility exhibit unique properties including absorbance, fluorescence, electrocatalytic activities, toxicity and QY, which are crucial for their practical applications, especially for the biological applications, as well as will lead our discussion in this part.

3.1. Absorbance

MoS_2 QDs showed non-obvious optical absorption in the ultraviolet-visible (UV-vis) absorption spectra, and only shoulder peaks at about 300 nm, which is the excitonic features of MoS_2 QDs that can be observed at UV region owing to quantum confinement effect [29, 30]. For example, MoS_2 QDs synthesized from ultrasonication and ethanol-thermal treatment displayed a shoulder peak at around 277 nm due to the blue-shifted convoluted Z, C, and D excitonic peaks [17]. Nevertheless, the MoS_2 QDs produced from Li intercalation exhibited absorption peak at 291 nm [31]. And new near-UV absorption peak at 300 nm was observed in the UV-Vis absorption spectra of MoS_2 QDs prepared from hydrothermal method [32]. The MoS_2 QDs fabricated from a combined method of sonication and ion intercalation in an alkaline environment displayed blue-shift compared with the nanosheets, and the peaks at 610 nm and 670 nm of MoS_2 nanosheets disappeared, which may be ascribed to quantum confinement effect (**Figure 6A**) [18]. The MoS_2 QDs from hydrothermal treatment of ammonium molybdate, thiourea and NAC exhibited three characteristic

absorption bands at about 264 nm, 313 nm and 380 nm (**Figure 6B**). The absorption bands at 380 nm and 313 nm may be ascribed to the excitonic absorption bands A and B, produced by the direct bandgap transition at K point with energy split from valence band spin-orbital coupling (**Figure 6C**) [26]. GSH-MoS_2 QDs prepared from solvothermal decomposition of ammonium tetrathiomolybdate and subsequent modification by GSH exhibited relatively high absorbance in the near-infrared (NIR) region with a mass extinction coefficient of 15.7 L/(g·cm) at 800 nm, showing the potential applications in photothermal cancer therapy (**Figure 6D**) [33]. The results reveal that the absorbance of MoS_2 QDs varies with the synthetic approaches.

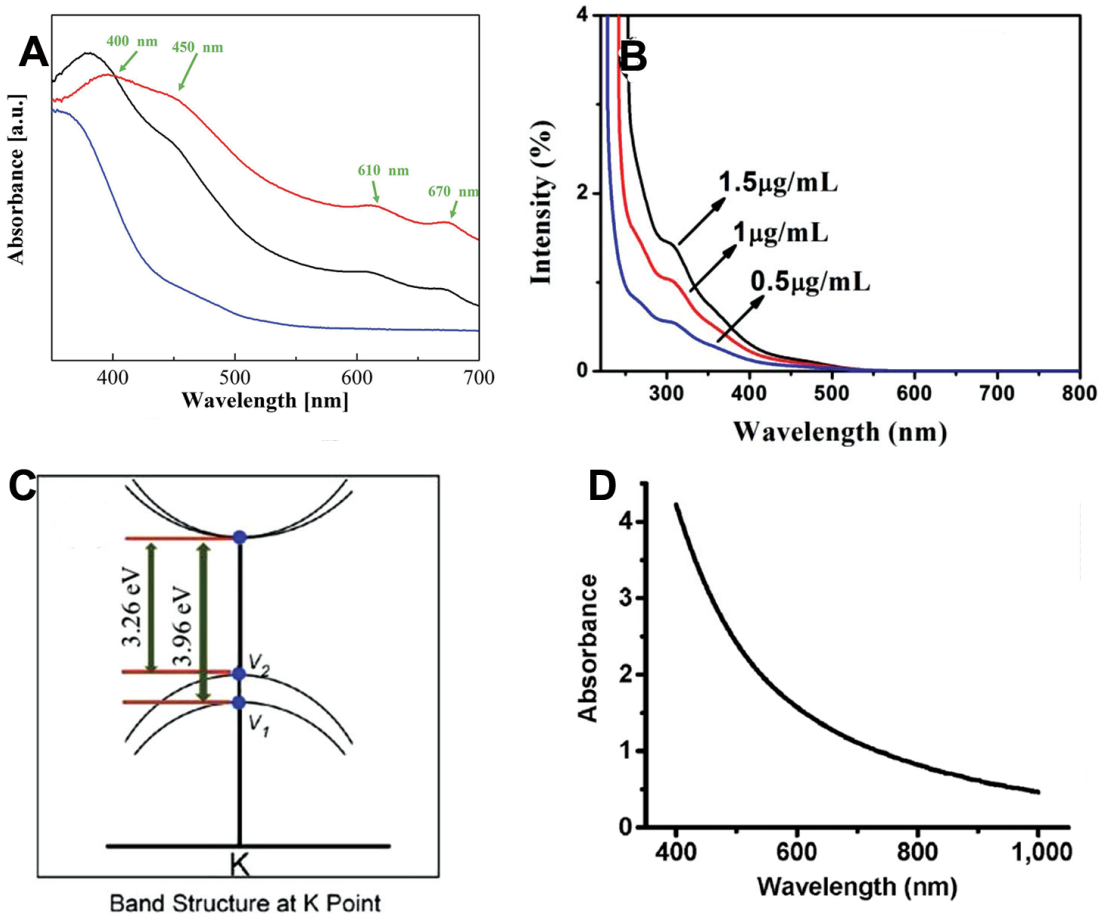

Figure 6. (A) UV-vis absorption spectra of large-sized MoS_2 nanosheets (red line), small-sized MoS_2 nanosheets (black line) and MoS_2 QDs (blue line). Reprinted with permission from [18]. Copyright (2015) the Royal Society of Chemistry. (B) UV-Vis absorption spectra of MoS_2 QDs in aqueous solutions with different concentration. (C) Diagram of the band structure of MoS_2 QDs close to the K point. B and C: Reprinted

with permission from [26]. Copyright (2015) Wiley-VCH. (D) UV-vis-NIR absorbance spectrum of the GSH-MoS_2 QDs solution. Reprinted with permission from [33]. Copyright (2016) Springer.

3.2 Fluorescence

Fluorescence is another essential property of MoS_2 QDs for potential applications in wide fields. Most of MoS_2 QDs exhibited blue emission under the excitation of UV light (365 nm), and the QY differed from the synthetic methods. Up to now, the real fluorescence mechanism of MoS2 QDs was not clearly elucidated, however, the fluorescence may be ascribed to the direct excitonic transitions between the minimum of conduction band and the maxima of split valence bands [26]. Cao and co-workers presented a simple hydrothermal method for synthesizing blue-emitting MoS_2 QDs with 12.7% using GSH as the reductant [32]. However, L-Cys-stabilized MoS_2 QDs prepared from hydrothermal method also showed blue emission, and the QY is only 2.6% [20]. Interestingly, Zhang's group has found that the fluorescence emission was dependent on the size of MoS_2 QDs. The fluorescence emission peak displayed an obvious red shift from 430 nm to 610 nm when the size increased from 2.0 nm to 7.0 nm [28]. And most MoS_2 QDs displayed excitation-dependent fluorescence behavior due to the polydispersity of MoS_2 QDs, hot fluorescence from the K point of the Brillouin zon, presence of surface defects and edge sites [20, 34]. Recently, a sonication combined with ion intercalation method has been developed to prepare MoS_2 QDs with variable fluorescence emission. The size of MoS_2 QDs varied from 1.5 nm to 7 nm with an average size of 3.5 nm. The fluorescence emission spectra of MoS_2 QDs exhibited an obvious red-shift from about 470 nm to 570 nm when excited under different wavelengths ranging from 320 nm to 520 nm. Thus, MoS_2 QDs could emit different fluorescence under different excitation wavelengths, demonstrating their promising applications in bioimaging field and optoelectronic devices (**Figure 7A**) [18].

Two-photon fluorescence imaging exhibits promising applications in biological fields due to the merits of minimized tissue autofluorescence, large penetration depth, high spatial resolution and reduced photodamage in biosystems [35]. MoS_2 QDs

prepared from one-step solvothermal method were found to display two-photon fluorescence property with two-photon fluorescence emission at 428 nm under excitation at 690 nm, which have been successfully applied for two-photon fluorescence imaging in MDA-MB-468 cells [17]. Interestingly, Dai and co-workers developed a sulfuric acid-assisted ultrasonic strategy for fabrication MoS_2 QDs with multiphoton fluorescence property, which was utilized for cell imaging with excitation of NIR excitation (700 nm) [10]. In addition, upconversion fluorescence was also observed in NAC-stabilized MoS_2 QDs prepared from a hydrothermal method, which was ascribed to the two successive energy transfers from the NIR absorption generated by the capping reagent NAC to MoS_2 QDs. With the increase of excitation wavelength, the upconversion fluorescence emission spectra displayed obvious red-shift (**Figure 7B**) [26]. Also, MoS_2 QDs displayed electrochemiluminescence property. Recently, Yuan's group found that MoS_2 QDs encapsulated Pd-Au convex hexoctahedrons composite showed electrochemiluminescence (ECL) with maximum ECL emission wavelength at 625 nm in the presence of triethylamine due to the electronic injection into a surface trap within the band gap of MoS_2 QDs [36].

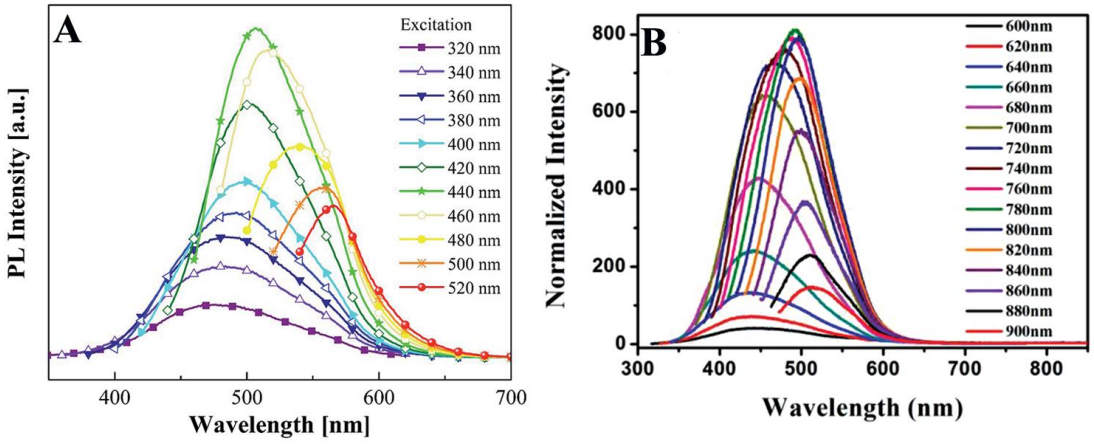

Figure 7. (A) Fluorescence emission spectra of MoS_2 QDs at different excitation wavelengths. Reprinted with permission from [18]. Copyright (2015) the Royal Society of Chemistry. (B) Upconversion fluorescence emission spectra of MoS_2 QDs with various excitation wavelengths. Reprinted with permission from [26]. Copyright (2015) Wiley-VCH.

3.3 Electrocatalytic activity

Similar to other two-dimensional nanomaterials, MoS_2 QDs also showed electrocatalytic properties. Ren *et al.* developed a hydrothermal method to synthesize MoS_2 QDs with electrocatalytic activities in the hydrogen evolution reaction (HER). The MoS_2 QDs with monolayer thickness of about 3.6 nm showed excellent catalytic activities with a low overpotential of approximately 160 mV and a small Tafel slope of 59 mV dec^{-1} due to the excellent intrinsic conductivity of the monolayer structure and abundance of exposed catalytic edge sites, demonstrating that the promising applications of the as-prepared MoS_2 QDs in HER [22]. MoS_2 QDs could be interspersed in few-layered sheets of MoS_2 based on a liquid exfoliation technique in organic solvents. The resulting MoS_2 nanostructures exhibited excellent electrocatalytic activity with low overpotential, which could be fabricated into electrodes for HER [37]. However, the electrocatalytic activity of MoS_2 QDs needs to be further investigated.

3.4 Toxicity

MoS_2 QDs are promising graphene-analogous transition-metal dichalcogenide nanomaterials with good biocompatibility, whose toxicity has been demonstrated by lots of research groups. Zhou and co-workers evaluated the toxicity of MoS_2 QDs prepared from a top-down route with methylthiazoleterazolium (MTT) assay. Surprisingly, MoS_2 QDs showed no significant cytotoxicity to HeLa cells and RAW 264.7 cells when the concentration was as high as 200 μg/mL, revealing the low toxicity of the as-prepared MoS_2 QDs [7]. Also, GSH-modified MoS_2 QDs (GSH-MoS_2 QDs) synthesized from one-step solvothermal decomposition of ammonium tetrathiomolybdate exhibited low toxicity from the results of MTT assay. After incubation of 4T1 murine breast cancer cells with GSH-MoS_2 QDs for 24 h, there was no obvious cytotoxicity even at the highest concentration of 200 μg/mL (**Figure 8A**). Meanwhile, reactive oxygen species and potential cell membrane damage were not generated by the as-synthesized GSH-MoS_2 QDs in 4T1 murine breast cancer cells (**Figure 8B**), suggesting that the excellent biocompatibility of the

MoS_2 QDs [33]. However, the long-term toxicity in vivo of MoS_2 QDs should been further evaluated.

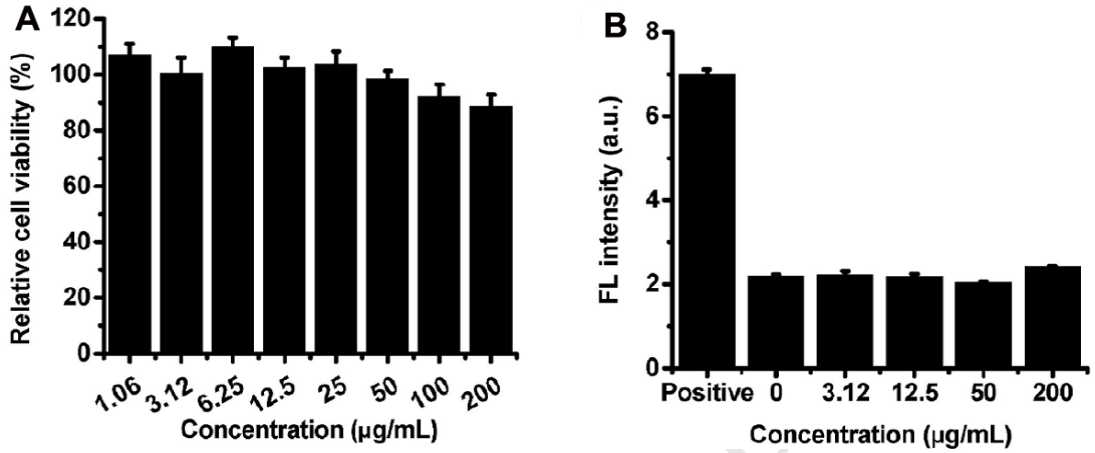

Figure 8. (A) Relative viabilities of 4T1 cells tested by the MTT assay after incubation with different concentrations of GSH-MoS_2 QDs for 24 h. (B) ROS signals of 4T1 cells after incubation with GSH-MoS_2 QDs at different concentrations. Reprinted with permission from [33]. Copyright (2016) Springer.

3.5 Quantum yield

QY is a crucial feature of MoS_2 QDs for the practical applications, especially in fluorescence sensing and cell imaging. The QY of MoS_2 QDs varies with the fabrication methods and the surface chemistry. The MoS_2 QDs resulted from the Na intercalation chemical exfoliation method showed blue emission with a high QY of 11% [7]. However, the QY of blue-emitting MoS_2 QDs prepared from sodium molybdate and L-Cys via a hydrothermal method was observed to be 2.6% [20]. And the MoS_2 QDs from the reduction of sodium molybdate with GSH under hydrothermal conditions displayed the QY of 12.7 % [32]. As mentioned above, most MoS_2 QDs exhibited lower QY when compared with that of carbon quantum dots [38]. It is, thus, highly pressing to develop much brighter MoS_2 QDs.

4. Biological applications

Currently, MoS_2 QDs have been demonstrated in a variety of fields owing to their above-mentioned unique properties. Among these applications, biological applications are one of the most important applications of MoS_2 QDs because the biological applications may have positive effects for human health or the environment.

In the following section, we have summarized the biological applications of MoS_2 QDs in biosensing, bioimaging, phototherapy and drug delivery.

4.1. Biosensing

The excellent properties make MoS_2 QDs as promising candidates for detecting various targets including metal ions, small biomolecules and biomacromolecules. In these biosensors, MoS_2 QDs can act as either electron donors or electron acceptors, the presence of targets can lead to fluorescence turn-off or turn-on of MoS_2 QDs. As a result, the MoS_2 QDs-based biosensors have been constructed.

Exposure of excess metal ions can cause serious harms to human health and the environment [38]. Cao *et al*. prepared MoS_2 QDs *via* a hydrothermal method with GSH as the reductant. The as-prepared MoS_2 QDs emitted blue-green fluorescence, which could be selectively quenched by Au(III) ions owing to the reduction of Au(III) and the deposition of Au(0) on the surface of the MoS_2 QDs. Accordingly, MoS_2 QDs could be utilized to determine Au(III) ions with the linear range from 0.5 to 1000 μM and limit of detection (LOD) of 64 nM [32]. Recently, Wang's group has fabricated MoS_2 QDs for detecting Pb^{2+} and S^{2-}. They found that Pb^{2+} could enhance the fluorescence of MoS_2 QDs because of the decrease of electron concentration caused by the formation of $PbSO_4$ on the surface of MoS_2 QDs. Taking advantage of the enhancement effect, a linear relationship within 0.5-12.0 μM was obtained for Pb^{2+} detection, and the LOD was 0.22 μM. Additionally, the enhancement effect could be selectively removed by the addition of S^{2-} due to the formation of PbS, which could increase the electron concentration MoS_2 QDs, resulting in fluorescence turn-off. As a result, the Pb^{2+}-doped MoS_2 QDs could be employed for sensing S^{2-} with a good linear relationship from 0.5 to 12.0 μM and the LOD of 0.42 μM (**Figure 9A**) [23].

MoS_2 QDs have been also used for detecting explosives based on the fluorescence turn-off mechanism. Wang and Ni have designed a selective fluorescence turn-off nanosensor for 2,4,6-trinitrophenol (TNP) using L-Cys-MoS_2 QDs based on the resonance energy transfer, electronic energy transfer, and electrostatic interactions between MoS_2 QDs and TNP. As a result, MoS_2 QDs showed an excellent sensitivity for TNP with the LOD of as low as 95 nM and a

linear response range of 0.099-36.5 μM (**Figure 9B**) [20]. Similarly, 4-diaminobutane-capped MoS_2 QDs have been constructed to sense TNP with the selectivity of 90% and LOD of 2.04 ppm. The high selectivity is due to electron transfer and Forster resonance energy transfer between MoS_2 QDs and TNP [25]. However, the linear relationship was not achieved. L-Cys- and GSH-stabilized MoS_2 QDs with blue emission have been prepared for fluorescence turn-off detection of tetracycline (TC), respectively. The L-Cys-MoS_2 QDs exhibited a linear response to the concentration of TC of 0-16 μM, and the LOD was 7.86 μM. The GSH-MoS_2 QDs displayed similar performance with a linear response range of 0-18 μM and the LOD of 6.52 μM. The detection mechanism may be attributed to the static quenching and inner filter effect (IFE) [39]. L-Cys-MoS_2 QDs were prepared for detecting methyl parathion (MP) based on the fluorescence turn-off mechanism caused by the IFE. In the detection system, the rapid hydrolysis of MP under alkaline conditions produced p-nitrophenol (p-NP). The spectral overlap of L-Cys-MoS_2 QDs emission spectra and the absorption spectra of p-NP promoted the fluorescence quenching. As a result, sensitive detection of MP was achieved with a linearity ranging from 0.1 to 30 μg/mL and a LOD of 0.085 μg/mL. Additionally, the method was successfully applied to determine the MP levels in rice and tap water [40].

Zhang's group synthesized GSH-MoS_2 QDs for the fluorescence turn-off detection of hydrogen peroxide (H_2O_2) and glucose in aqueous solution. The oxidation of GSH-MoS_2 QDs by H_2O_2 could lead to the fluorescence quenching, resulting in the selective analysis of H_2O_2 with a good linear relationship in the range of 50 μM-1.2 mM. By combining glucose oxidase with GSH-MoS_2 QDs, detection of glucose could be achieved due to the production of H_2O_2 caused by the oxidation of glucose catalyzed by glucose oxidase. As a result, a good linear relationship was obtained in the glucose concentration range from 0 to 1.5 mM with a LOD of 5.16 μM. Moreover, the GSH-MoS_2 QDs was successfully applied to sense glucose in fetal bovine serum samples (**Figure 9C**) [21]. Interestingly, Karthikeyan's group has found that glucose and bovine serum albumin (BSA) could enhance fluorescence of L-Cys-MoS_2 QDs because of the band bending effect. As a result, a performance for

the detection of glucose and BSA with the linear range between 30 nM and 300 nM was achieved. Also, the L-Cys-MoS_2 QDs exhibited good selectivity towards glucose and BSA, except human serum albumin (HSA) [41].

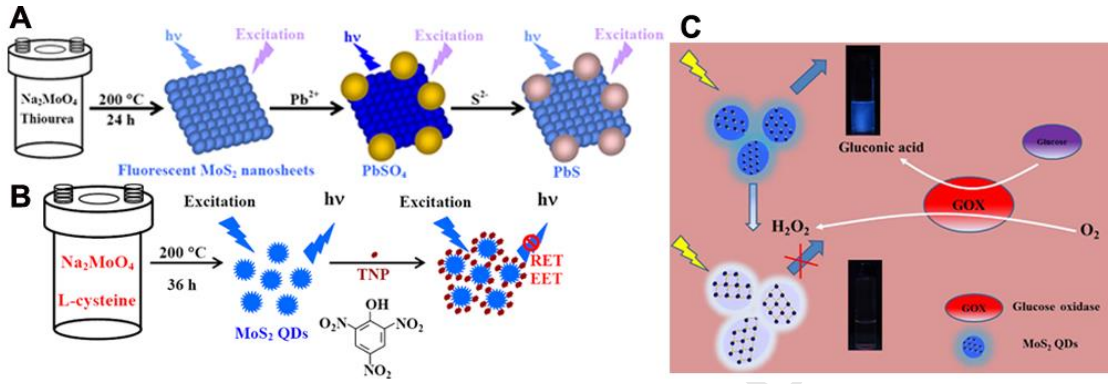

Figure 9. (A) Illustration of synthesis of MoS_2 QDs and fluorescence sensing of Pb^{2+} and S^{2-}. Reprinted with permission from [23]. Copyright (2016) American Chemical Society. (B) Scheme of preparation of MoS_2 QDs and fluorescence sensing of TNP. Reprinted with permission from [20]. Copyright (2014) American Chemical Society. (C) Schematic representation of MoS_2 QDs for fluorescence sensing of H_2O_2 and glucose. Reprinted with permission from [21]. Copyright (2017) Elsevier.

Surprisingly, MoS_2 QDs could be combined with MnO_2 nanosheets to construct a fluorescence turn-on nanosensor for the determination of ascorbic acid (AA). In the nanosensor, the fluorescence of MoS_2 QDs could be suppressed by MnO_2 nanosheets due to IFE, yet the presence of AA could restore the fluorescence of MoS_2 QDs because AA could reduce MnO_2 nanosheets into Mn^{2+}. Consequently, sensitive detection of AA was realized with the linear range from 0.33 μM to 5.00 μM and the LOD of 39 nM (**Figure 10A**). Importantly, the AA levels in hawthorn and jujube was successfully determined with the nanosensor [42]. Xu *et al*. have synthesized thioglycollic acid stabilized MoS_2 QDs (TGA-MoS_2 QDs) via a hydrothermal method. They found that dopamine (DA) could selectively quench the fluorescence of MoS_2 QDs, which was ascribed to the charge transfer caused by the stacking of MoS_2 QDs through C-O···H-O hydrogen bonding interaction. Accordingly, DA was selectively and rapidly determined with the linear range of 0.05-20 μM and the LOD of 27 nM. The as-prepared TGA-MoS_2 QDs were successfully employed to detect DA levels in

urine and serum sample with a good recovery [24]. Tseng's group recently found 6-mercaptopurine (6-MP) could quench the fluorescence of MoS_2 QDs because of the acceptor-excited photoinduced electron transfer caused by the occupation of sulfur vacancies by 6-MP. Interestingly, the addition of GSH could trigger the release of 6-MP from the MoS_2 QDs, accompanying with the fluorescence turn-on of MoS_2 QDs. Thus, the detection of GSH could be realized with 6-MP-MoS_2 QDs with a wider linear range of 0.1-100 μM and 0.1-4 mM, and the LOD was approximately 30 nM. The 6-MP-MoS_2 QDs were successfully applied to selectively sense GSH in HeLa cells and erythrocytes [34].

Gu and coworkers have employed MoS_2 QDs as fluorescent probes for hyaluronidase (HAase) detection. Hyaluronic acid-functionalized gold nanoparticles (HA-AuNPs) could quench the fluorescence of MoS_2 QDs via a photoinduced electron-transfer mechanism. HAase is an endoglucosidase, which could cleave HA into proangiogenic fragments and cause the aggregation of AuNPs, resulting in the fluorescence recovery owing to the blockage of electron transfer. Under the optimized experimental conditions, a linear range of 1-50 U/mL and a LOD of 0.7 U/mL for HAase detection was achieved (**Figure 10B**). Moreover, the approach was demonstrated in human urine with a good recovery [27].

MoS_2 QDs could be combined with graphene oxide (GO) and reduced graphene oxide (RGO) to fabricate nanosensors for the fluorescence turn-on detection of BSA and HSA. The fluorescence of MoS_2 QDs could be quenched by GO and RGO due to the excited-state electron transfer and/or energy transfer. Still, the addition of BSA or HSA could recover the fluorescence of MoS_2 QDs because of the reduction of transfer of electrons and storage of excess electrons from MoS_2 QDs caused by the noncovalent π-π stacking between BSA/HSA and GO or RGO. As a result, BSA/HAS was sensitively determined with the linear relationship ranging from 5 nM to 50 nM [43].

As discussed above, a large number of examples of MoS_2 QDs have been applied to detect various analytes (**Table 2**). However, most of the responsive mechanisms of MoS_2 QDs for biosensing are fluorescence turn-off and the fluorescence signal is

easily disturbed by other factors. Novel detection mechanism with more accuracy is, therefore, highly desirable.

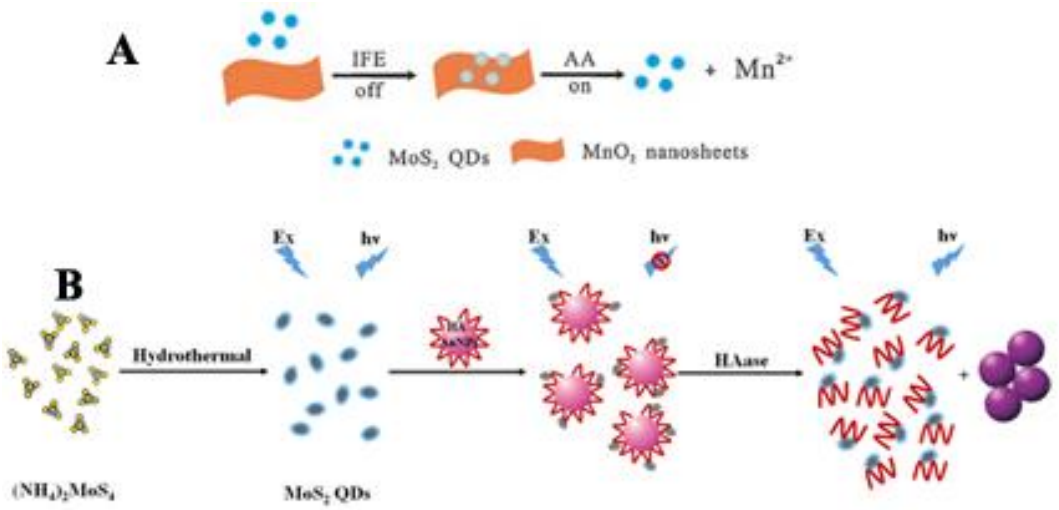

Figure 10. (A) Scheme of MoS_2 QDs-MnO_2 system for sensing ascorbic acid. Reprinted with permission from [42]. Copyright (2017) Elsevier. (B) Illustration of synthesis of MoS_2 QDs and MoS_2 QDs as fluorescent probes for detection of HAase. Reprinted with permission from [27]. Copyright (2016) American Chemical Society.

Table 2 Comparison of the performance of MoS_2 QDs for biosensing.

Target	Probes	Fluorescence response	Linear range	Limit of detection	Reference
Au^{3+}	GSH-MoS_2 QDs	Fluorescence turn-off	0.5-1000 μM	64 nM	[32]
Pb^{2+}	MoS_2 QDs	Fluorescence turn-on	0.5-12.0 μM	0.22 μM	[23]
S^{2-}	MoS_2 QDs	Fluorescence turn-off	0.5-12.0 μM	0.42 μM	[23]
2,4,6-Trinitrophenol	L-cysteine-MoS_2 QDs	Fluorescence turn-off	0.099-36.5 μM	95 nM	[20]
2,4,6-trinitrophenol	4-diaminobutane-MoS_2 QDs	Fluorescence turn-off	-	2.04 ppm	[25]
Tetracycline	L-cysteine-MoS_2 QDs	Fluorescence turn-off	0-16 μM	7.86 μM	[39]
Tetracycline	GSH-MoS_2 QDs	Fluorescence turn-off	0-18 μM	6.52 μM	[39]
Methyl parathion	L-cysteine-MoS_2 QDs	Fluorescence turn-off	0.38-114.0 μM (0.1-30 μg/mL)	0.32 μM (0.085 μg/mL)	[40]
H_2O_2	GSH-MoS_2 QDs	Fluorescence turn-off	50 μM-1.2 mM	-	[21]
Glucose	GSH-MoS_2 QDs	Fluorescence turn-off	0-1.5 mM	5.16 μM	[21]
Glucose, BSA	L-cysteine-MoS_2 QDs	Fluorescence enhancement	30-300 nM	-	[41]
Ascorbic acid	GSH-MoS_2 QDs/MnO_2 nanosheets	Fluorescence turn-on	0.33-5.00 μM	39 nM	[42]
Dopamine	Thioglycollic acid-MoS_2 QDs	Fluorescence turn-off	0.05-20 μM	27 nM.	[24]
GSH	6-mercaptopurine-MoS_2	Fluorescence turn-on	0.1-100 μM,	30 nM.	[34]

	QDs		0.1-4 mM		
Hyaluronidase	MoS_2 QDs/hyaluronic acid-AuNPs system	Fluorescence turn-on	1-50 U/mL	0.7 U/mL	[27]
BSA/HSA	L-cysteine-MoS_2 QDs /GO or RGO	Fluorescence turn-on	5-50 nM		[43]

4.2. Bioimaging

Bioimaging is another promising application of MoS_2 QDs due to their excellent fluorescence properties and low toxicity. Zhou *et al*. have synthesized highly fluorescent MoS_2 QDs with excellent photostability and low cytotoxicity. The as-prepared MoS_2 QDs could be stained HeLa cells and still remained bright fluorescence even for 48 h after the cell culture, demonstrating that the MoS_2 QDs could be used for long-term tracing live cells, which might be ascribed to the fact that the defect sites on MoS_2 QDs can be passivated by thiol-containing species in live cells [7]. Zhang *et al*. have synthesized highly fluorescent MoS_2 QDs with variable photoluminescence emission. The as-prepared MoS_2 QDs exhibited an excitation-dependent emission behavior, suggesting that the MoS_2 QDs could emit different fluorescence under different excitation wavelengths, which have further been utilized for cell imaging. The MoS_2 QDs internalized by the lung cells could emit different colors of fluorescence by altering the excitation wavelength, and these MoS_2 QDs did not penetrating the nuclei, indicating that MoS_2 QDs have the low toxicity and promising applications in biomedicine (**Figure 11**) [18].

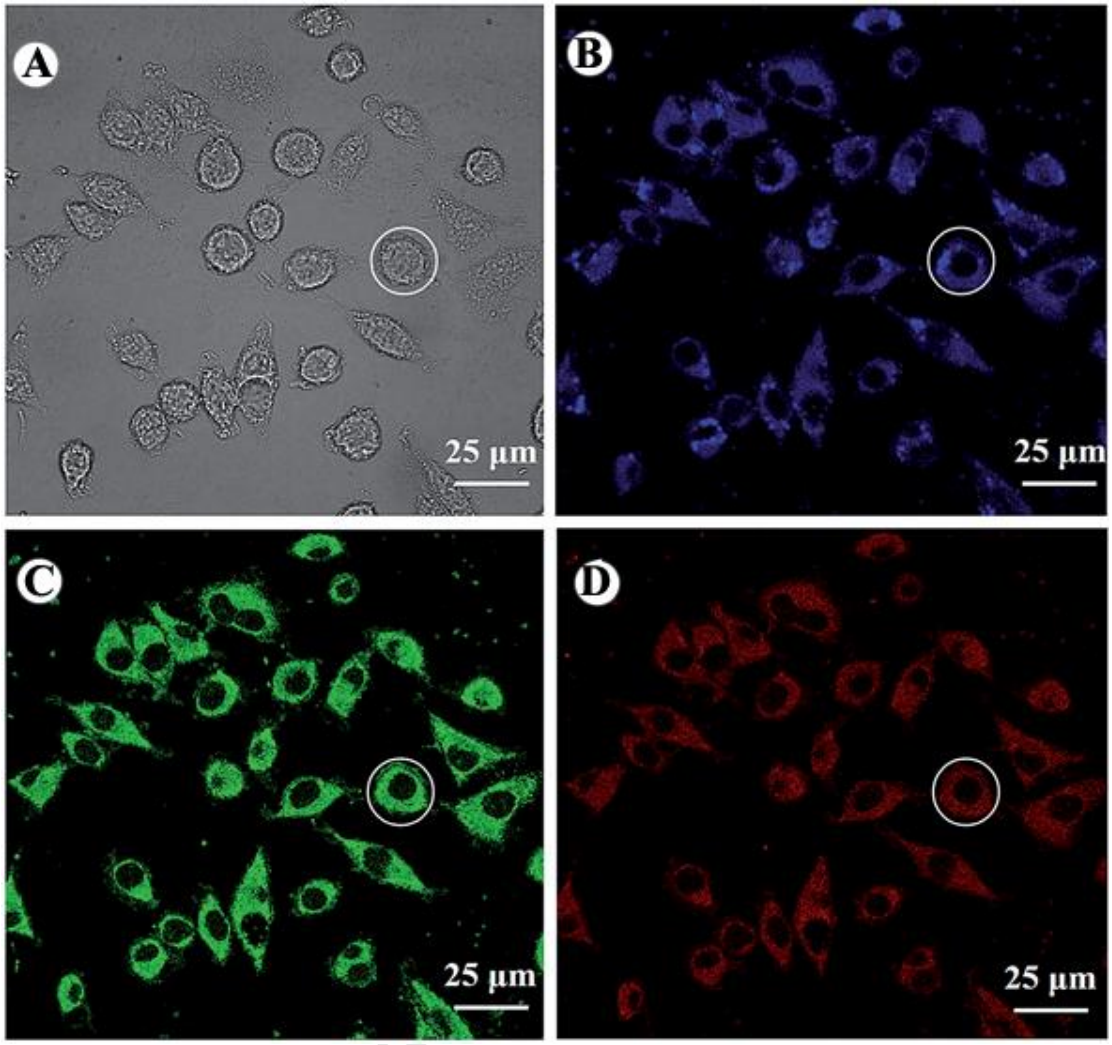

Figure 11. (A) Bright field image of MoS_2 QDs with human lung cells. (B to D) Fluorescent images of cells imaged under excitation light with the wavelength of 405 nm, 488 nm and 552 nm, respectively. Reprinted with permission from [18]. Copyright (2015) the Royal Society of Chemistry.

Sweet *et al.* have prepared MoS_2 QDs displaying super high two-photon absorption (TPA) properties with a TPA cross-section of 58960 GM, which is much higher than that of semiconductor QDs and organic fluorescent dyes. After modification with anti-PSMA, the anti-PSMA/MoS_2 QDs could be employed for selective two-photon imaging of live prostate cancer cells with 1064 nm light that could not exhibit any serious damage to live cells, suggesting that the anti-PSMA/MoS_2 QDs can distinguish the targeted prostate cancer LnCaP cells from other nontargeted cells [44]. Zhang's group has fabricated MoS_2 QDs for multiphoton

cell imaging. MoS_2 QDs were introduced into HeLa and HaCaT cells, and the blue fluorescence could be easily observed with the excitation NIR light (700 nm). Also, the fluorescence brightness did not alter under continuous excitation over 30 min, revealing that the obtained MoS_2 QDs could be used for multiphoton bioimaging (**Figure 12**) [10].

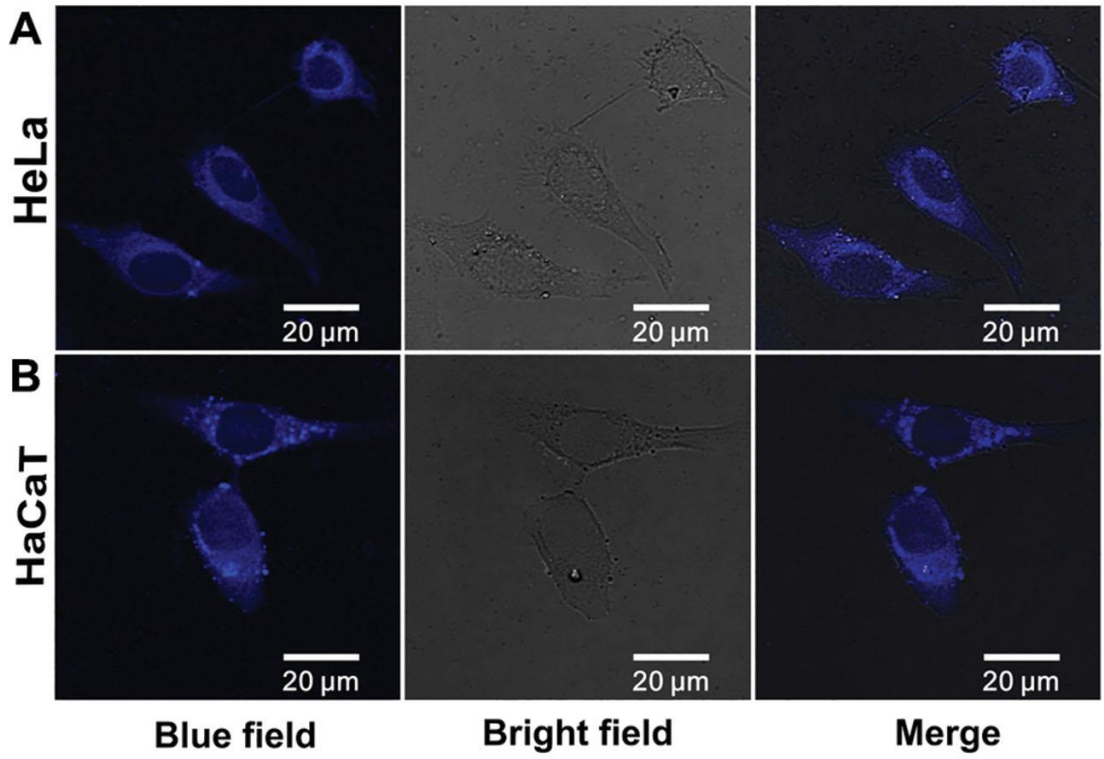

Figure 12. The multiphoton luminescence images of (A) HeLa and (B) HaCaT cells with MoS_2 QDs. Excitation wavelength was 700 nm and detection wavelength was in the 420-460 nm range. Reprinted with permission from [10]. Copyright (2015) the Royal Society of Chemistry.

4.3 Phototherapy

Phototherapy is an effective approach for the treatment of cancers. Considering that MoS_2 QDs own specific optical properties, scientists have also utilized them as photothermal agents for the phototherapy to cancers. Liu's group prepared ultra-small MoS_2 QDs via a one-step solvothermal decomposition of ammonium tetrathiomolybdate. After modification of GSH, the GSH-modified MoS_2 QDs (GSH-MoS_2 QDs) exhibited high stability in physiological conditions, strong fluorescence and low toxicity. The GSH-MoS_2 QDs have long blood circulation

half-life and could maximally accumulate in tumors after intravenous (*i.v.*) injection for 4 h, which could be monitored by photoacoustic (PA) imaging. And the GSH-MoS_2 QDs can be easily cleared via urine due to their ultra-small hydrodynamic size. Most importantly, the GSH-MoS_2 QDs showed strong NIR absorbance, which could be used to induce remarkable photothermal ablation of cancer cells. After *i.v.* injecting each mouse with 200 μL GSH-MoS_2 QDs at a concentration of 0.5 mg/mL for four hours, 808 nm laser at a power density of 1 W/cm^2 was employed to irradiate the mouse for 5 min. The tumors of the mice injected with GSH-MoS_2 QDs were completely eradicated without recurrence [33]. However, the absorption efficiency of MoS_2 QDs for NIR is not perfect. To improve the performance of MoS_2 QDs, MoS_2 QDs@polyaniline (MoS_2@PANI) inorganic-organic nanohybrids were designed for enhancing PA imaging/X-ray computed tomography (CT) and efficient radiotherapy (RT)/photothermal therapy (PTT) of cancer. MoS_2 QDs were first synthesized through a simple solvothermal method and were dispersed in PVP aqueous solution. Aniline and 3-aminobenzoic acid (aniline-COOH) with a certain molar ratio polymerized on the surface of MoS_2 QDs with the assistance of ammonium persulfate. Then, PEG-NH_2 was then covalently conjugated to the surface of MoS_2@PANI-COOH nanoparticles, yielding the stable and soluble MoS_2@PANI-PEG nanohybrids, which displayed a broad absorption peak in the NIR region and bright fluorescence with longer wavelength when compared with the original MoS_2 QDs. The MoS_2@PANI-PEG nanohybrids showed good NIR light-evoked photothermal effect and great photostability, making them as good candidates for treating cancer. As a result, simultaneous CT/PA imaging and synergistic PTT/RT combination therapy for cancer in vitro and in vivo were successfully accomplished owing to their good biocompatibility (**Figure 13**) [45]. Surprisingly, a sort of MoS_2 QDs prepared from tetrabutylammonium-assisted ultrasonication of multilayered MoS_2 powder exhibited excellent $^1O_2$ production ability, which is even better than that of the commercial photosensitizer PpIX, revealing that the as-prepared MoS_2 QDs are promising for photodynamic therapy [30].

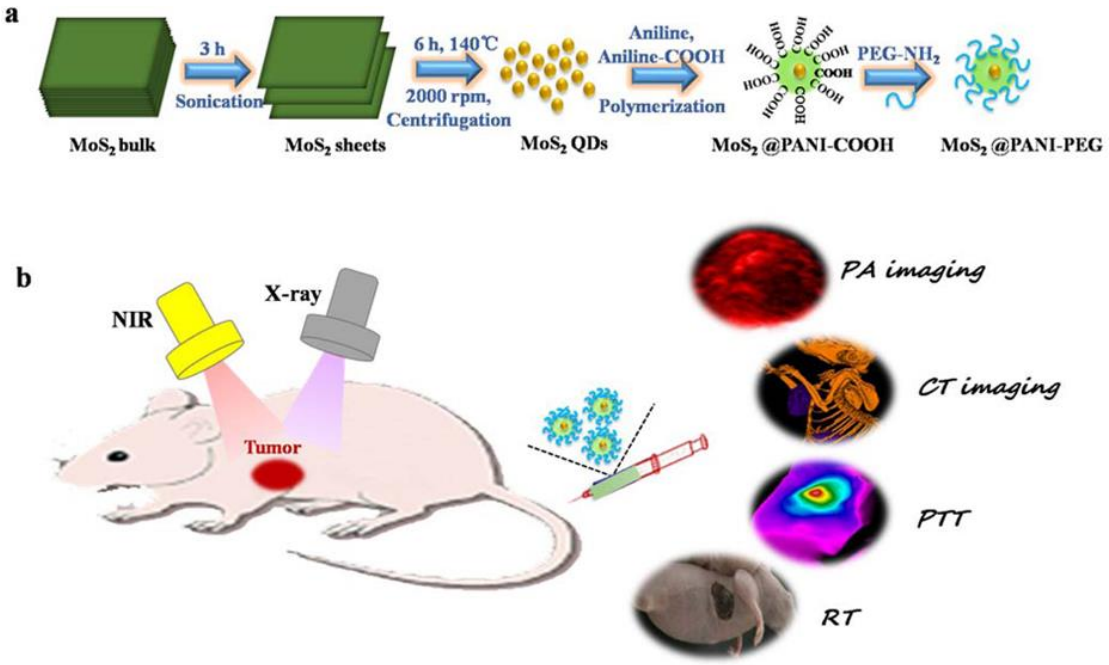

Figure 13. Schematic representation of the synthesis of MoS_2@PANI-PEG nanohybrids and the applications of MoS_2@PANI-PEG nanohybrids for dual modal imaging and combined PTT and RT therapy. Reprinted with permission from [45]. Copyright (2016) American Chemical Society.

4.4 Drug delivery

In recent years, a variety of quantum dots have been utilized as nanocarriers for drug delivery due to their bright photoluminescence, good biocompatibility and rapid cellular uptake [36-38]. MoS_2 QDs have been prepared through ultrasonication assisted liquid exfoliation and solvothermal treatment of layered materials in dimethylformamide. The obtained MoS_2 QDs were combined with hydrophobic thiolated doxorubicin (DOX-SH) to form DOX-SH/M-MoS_2 QDs, in which DOX-SH could be chemically adsorbed at the sulfur vacancy sites of the M-MoS_2 QDs. The DOX-SH/M-MoS_2 QDs displayed efficient uptake by HeLa cells and greater cytotoxicity than free DOX-SH and DOX owing to the release of DOX-SH triggered by GSH in HeLa cells. Meanwhile, fluorescence imaging was used to monitor *in vivo* release of DOX in mice [34]. MoS_2 QDs exhibited great potential for delivering thiol-containing cancer drugs, nevertheless, the applications of MoS_2 QDs as platforms for delivery drugs are needed to be further demonstrated.

5. Conclusion and outlook

The past decades have witnessed the rapid development of synthesis of MoS_2 QDs and biological applications. However, there are still several challenges in the preparation and biological applications. Firstly, novel synthetic approaches for MoS_2 QDs with high quantum yield and longer fluorescence emission wavelength should be further developed because most of present MoS_2 QDs exhibit low QY and blue emission, which may exert negative effects on the biological system during the biological applications. Also, facile and simple strategies should be explored due to the fact that the presented methods are complicated and energy-consuming, which are not appropriate for large-scale production of MoS_2 QDs. Secondly, novel properties of MoS_2 QDs are highly desirable because new applications are related with novel properties. Thirdly, most of the present MoS_2 QDs-based biosensors are fluorescence turn-off, and the fluorescence signal is easily influenced by the detection system, which may result in incorrect detection results. Thus, novel detection mechanisms, such as fluorescence turn-on or ratiometric response, should be demonstrated in biosensing applications to improve the accuracy of detection results. Last but not the least, the biological applications of MoS_2 QDs should be further widened and deepened in more fields including biomedicine, environment, and food. With the rapid development of nanotechnology, much brighter MoS_2 QDs will be fabricated and the biological applications with more robustness will be explored.

Acknowledgements

The work was financially supported by The Startup Foundation for Introducing Talent of NUIST (2018r056), the National Natural Science Foundation of China (21401113), the Finnish Culture Foundation, the University of Turku, the Natural Science Foundation of Henan Department of Science & Technology (172102310668).

REFERENCES

[1] J. Ping, Z. Fan, M. Sindoro, Y. Ying, H. Zhang, Recent advances in sensing applications of two-dimensional transition metal dichalcogenide nanosheets and their composites, Adv. Funct. Mater. 27 (2017) 1605817.

[2] E. Singh, K.S. Kim, G.Y. Yeom, H.S. Nalwa, Two-dimensional transition metal dichalcogenide-based counter electrodes for dye-sensitized solar cells, RSC Adv. 7 (2017) 28234.

[3] C. Tan, H. Zhang, Two-dimensional transition metal dichalcogenide nanosheet-based composites, Chem. Soc. Rev. 44 (2015) 2713.

[4] L. Gong, L. Yan, R. Zhou, J. Xie, W. Wu, Z. Gu, Two-dimensional transition metal dichalcogenide nanomaterials for combination cancer therapy, J. Mater. Chem. B 5 (2017) 1873.

[5] V. Yadav, S. Roy, P. Singh, Z. Khan, A. Jaiswal, 2D MoS_2-based nanomaterials for therapeutic, bioimaging, and biosensing applications, Small 15 (2019) 1803706.

[6] N.S. Arul, V.D. Nithya, Molybdenum disulfide quantum dots: synthesis and applications, RSC Adv. 6 (2016) 65670.

[7] K. Zhou, Y. Zhang, Z. Xia, W. Wei, As-prepared MoS_2 quantum dot as a facile fluorescent probe for long-term tracing of live cells, Nanotechnology 27 (2016) 275101.

[8] W. Qiao, S. Yan, X. Song, X. Zhang, X. He, W. Zhong, Y. Du, Luminescent monolayer MoS_2 quantum dots produced by multi-exfoliation based on lithium intercalation, Appl. Surf. Sci. 359 (2015) 130.

[9] V. Stengl, J. Henych, Strongly luminescent monolayered MoS_2 prepared by effective ultrasound exfoliation, Nanoscale 5 (2013) 3387.

[10] W. Dai, H. Dong, B. Fugetsu, Y. Cao, H. Lu, X. Ma, X. Zhang, Tunable fabrication of molybdenum disulfide quantum dots for Intracellular microRNA detection and multiphoton bioimaging, Small 11 (2015) 4158.

[11] D. Gopalakrishnan, D. Damien, B. Li, H. Gullappalli, V.K. Pillai, P.M. Ajayan, M.M. Shaijumon, Electrochemical synthesis of luminescent MoS_2 quantum dots, Chem. Commun. 51 (2015) 6293.

[12] B.L. Li, L.X. Chen, H.L. Zou, J.L. Lei, H.Q. Luo, N.B. Li, Electrochemically induced Fenton reaction of few-layer MoS_2 nanosheets: preparation of luminescent quantum dots via a transition of nanoporous morphology, Nanoscale 6 (2014) 9831.

[13] N. Wang, F. Wei, Y. Qi, H. Li, X. Lu, G. Zhao, Q. Xu, Synthesis of strongly

fluorescent molybdenum disulfide nanosheets for cell-targeted labeling, ACS Appl. Mater. Interfaces 6 (2014) 19888.

[14] Q. Liu, C. Hu, X. Wang, A facile one-step method to produce MoS_2 quantum dots as promising bio-imaging materials, RSC Adv. 6 (2016) 25605.

[15] S. Xu, D. Li, P. Wu, One-pot, facile, and versatile synthesis of monolayer MoS2/WS2 quantum dots as bioimaging probes and efficient electrocatalysts for hydrogen evolution reaction, Adv. Funct. Mater. 25 (2015) 1127.

[16] S.J. Park, W.P. Sang, D. Qiu, J.H. Kang, D.Y. Song, E.K. Kim, Structural and optical characterization of MoS_2 quantum dots defined by thermal annealing, J. Lumin. 183 (2017) 62.

[17] G. Wei, Y. Yan, X. Cao, C. Zhang, C. Ding, Y. Xian, A facile and one-step ethanol-thermal synthesis of MoS_2 quantum dots for two-photon fluorescence imaging, J. Mater. Chem. B 4 (2016) 27.

[18] J.Y. Wu, X.Y. Zhang, X.D. Ma, Y.P. Qiu, T. Zhang, High quantum-yield luminescent MoS_2 quantum dots with variable light emission created via direct ultrasonic exfoliation of MoS_2 nanosheets, RSC Adv. 5 (2015) 95178.

[19] J. Ali, G.U. Siddiqui, K.H. Choi, Y. Jang, K. Lee, Fabrication of blue luminescent MoS_2 quantum dots by wet grinding assisted co-solvent sonication, J. Lumin. 169 (2016) 342.

[20] Y. Wang, Y. Ni, Molybdenum disulfide quantum dots as a photoluminescence sensing platform for 2,4,6-trinitrophenol detection, Anal. Chem. 86 (2014) 7463.

[21] X. Wang, Q. Wu, K. Jiang, C. Wang, C. Zhang, One-step synthesis of water-soluble and highly fluorescent MoS_2 quantum dots for detection of hydrogen peroxide and glucose, Sens. Actuators B: Chem. 252 (2017) 183.

[22] X. Ren, L. Pang, Y. Zhang, X. Ren, H. Fan, S. Liu, One-step hydrothermal synthesis of monolayer MoS_2 quantum dots for highly efficient electrocatalytic hydrogen evolution, J. Mater. Chem. A 3 (2015) 10693.

[23] Y. Wang, J. Hu, Q. Zhuang, Y. Ni, Label-free fluorescence sensing of lead(II) ions and sulfide ions based on luminescent molybdenum disulfide nanosheets, ACS Sustainable Chem. Eng. 4 (2016) 2535.

[24]B. Xu, Y. Su, L. Li, R. Liu, Y. Lv, Thiol-functionalized single-layered MoS_2 nanosheet as a photoluminescence sensing platform via charge transfer for dopamine detection, Sens. Actuators B: Chem. 246 (2017) 380.

[25]D. Haldar, D. Dinda, S.K. Saha, High selectivity in water soluble MoS_2 quantum dots for sensing nitro explosives, J. Mater. Chem. C 4 (2016) 6321.

[26]H. Huang, C. Du, H. Shi, X. Feng, J. Li, Y. Tan, W. Song, Water-soluble monolayer molybdenum disulfide quantum dots with upconversion fluorescence, Part. Part. Syst. Charact. 32 (2015) 72.

[27]G. Wei, Y. Yan, C. Zhang, C. Ding, Y. Xian, One-step synthesis of water-soluble MoS_2 quantum dots via a hydrothermal method as a fluorescent probe for hyaluronidase detection, ACS Appl. Mater. Interfaces 8 (2016) 11272.

[28]H. Lin, C. Wang, J. Wu, Z. Xu, Y. Huang, C. Zhang, Colloidal synthesis of MoS_2 quantum dots: size-dependent tunable photoluminescence and bioimaging, New J. Chem. 39 (2015) 8492.

[29]S. Zhang, X. Jia, E. Wang, Facile synthesis of optical pH-sensitive molybdenum disulfide quantum dots, Nanoscale 8 (2016) 15152.

[30]H. Dong, S. Tang, Y. Hao, H. Yu, W. Dai, G. Zhao, Y. Cao, H. Lu, X. Zhang, H. Ju, Fluorescent MoS_2 quantum dots: ultrasonic preparation, up-conversion and down-conversion bioimaging, and photodynamic therapy, ACS Appl. Mater. Interfaces 8 (2016) 3107.

[31]H.D. Ha, D.J. Han, J.S. Choi, M. Park, T.S. Seo, Dual role of blue luminescent MoS_2 quantum dots in fluorescence resonance energy transfer phenomenon Small 10 (2014) 3858.

[32]H. Cao, H. Wang, Y. Huang, Y. Sun, S. Shi, M. Tang, Quantification of gold(III) in solution and with a test stripe via the quenching of the fluorescence of molybdenum disulfide quantum dots, Microchim. Acta 184 (2017) 91.

[33]T. Liu, Y. Chao, M. Gao, C. Liang, Q. Chen, G. Song, L. Cheng, Z. Liu, Ultra-small MoS_2 nanodots with rapid body clearance for photothermal cancer therapy, Nano Res. 9 (2016) 3003.

[34]S.-C. Chen, C.-Y. Lin, T.-L. Cheng, W.-L.C. Tseng, 6-Mercaptopurine-induced

fluorescence quenching of monolayer MoS_2 nanodots: applications to glutathione sensing, cellular imaging, and glutathione-stimulated drug delivery, Adv. Funct. Mater. 27 (2017) 1702452.

[35] Y. Guo, F. Cao, X. Lei, L. Mang, S. Cheng, J. Song, Fluorescent copper nanoparticles: recent advances in synthesis and applications for sensing metal ions, Nanoscale 8 (2016) 4852.

[36] M. Zhao, A. Chen, D. Huang, Y. Chai, Y. Zhuo, R. Yuan, MoS_2 quantum dots as new electrochemiluminescence emitters for ultrasensitive bioanalysis of lipopolysaccharide, Anal. Chem. 89 (2017) 8335.

[37] D. Gopalakrishnan, D. Damien, M.M. Shaijumon, MoS_2 quantum dot-interspersed exfoliated MoS_2 nanosheets, ACS Nano 8 (2014) 5297.

[38] Y. Guo, L. Zhang, S. Zhang, Y. Yang, X. Chen, M. Zhang, Fluorescent carbon nanoparticles for the fluorescent detection of metal ions, Biosens. Bioelectron. 63 (2015) 61.

[39] Z. Wang, J. Lin, J. Gao, Q. Wang, Two optically active molybdenum disulfide quantum dots as tetracycline sensors, Mater. Chem. Phys. 178 (2016) 82.

[40] N. Fahimikashani, A. Rashti, M.R. Hormozinezhad, V. Mahdavi, MoS_2 quantum-dots as a label-free fluorescent nanoprobe for the highly selective detection of methyl parathion pesticide, Anal. Methods 9 (2017) 716.

[41] S. Hariharan, B. Karthikeyan, Optical and surface band bending mediated fluorescence sensing properties of MoS_2 quantum dots, RSC Adv. 6 (2016) 101770.

[42] Y.L. Xu, X.Y. Niu, H.L. Chen, S.G. Zhao, X.G. Chen, Switch-on fluorescence sensor for ascorbic acid detection based on MoS_2 quantum dots-MnO_2 nanosheets system and its application in fruit samples, Chinese Chem. Lett. 28 (2017) 338.

[43] H. Swaminathan, V. Ramar, K. Balasubramanian, Excited-state electron and energy transfer dynamics between 2D MoS_2 and GO/RGO for turn on BSA/HSA Sensing, J. Phys. Chem. C 121 (2017) 12585.

[44] C. Sweet, A. Pramanik, S. Jones, P.C. Ray, Two-photon fluorescent molybdenum disulfide dots for targeted prostate cancer imaging in the biological II window, ACS Omega 2 (2017) 1826.

[45]J. Wang, X. Tan, X. Pang, L. Liu, F. Tan, N. Li, MoS_2 quantum dots@polyaniline inorganic-organic nanohybrids for in vivo dual-modal imaging guided synergistic photothermal/radiation therapy, ACS Appl. Mater. Interfaces 8 (2016) 24331.

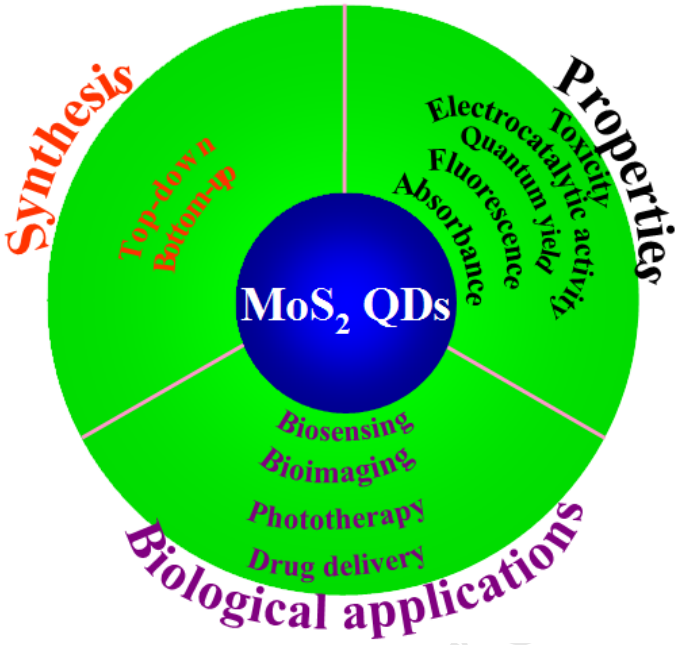

Graphical abstract

Highlights

- Significant advances of MoS_2 QDs in synthetic strategies, distinctive properties and detailed biological applications are presented.
- The challenges and perspectives of MoS_2 QDs based materials are indicated as well.